

Coherent Terahertz Emission Using Metasurfaces to Intercept a Flat Electron Beam

Zijia Yu^{1,‡}, Liwen Zhang,^{1,‡} Weihao Liu^{2,*†}, Jiapeng Yin,³ Yucheng Liu,¹ Qika Jia^{1,‡}, Baogen Sun,¹ Hongliang Xu,¹ and Shengguang Liu^{3,‡}

¹*National Synchrotron Radiation Laboratory, University of Science and Technology of China, Hefei, Anhui 230029, China*

²*College of Electronic and Information Engineering, Nanjing University of Aeronautics and Astronautics, Nanjing, Jiangsu 211106, China*

³*Key Laboratory for Laser Plasmas (Ministry of Education), Shanghai Jiao Tong University, Shanghai 200240, China*



(Received 19 April 2021; revised 5 December 2021; accepted 7 December 2021; published 27 January 2022)

Terahertz electromagnetic radiation is one of the hottest research topics thanks to its promising applications in diverse scientific and technological fields. Using a uniformly moving electron beam to interact with a metallic or dielectric surface is an efficient tool for the generation of high-power terahertz waves. In the present paper, we demonstrate enhanced coherent terahertz emission theoretically and experimentally by using a metasurface formed by an array of Fabry-Perot-like resonators to obliquely intercept a low-energy flat electron beam. We illustrate that the mechanism is one of modified coherent Smith-Purcell radiation rather than the expected transition radiation. More notably, this metasurface overcomes the inherent restriction imposed by the decay length in conventional beam-wave interactions, greatly enhancing the radiation efficiency and intensity. This emission promises an attractive way of developing high-power terahertz sources.

DOI: 10.1103/PhysRevApplied.17.014038

I. INTRODUCTION

The interaction of electron beams with metallic or dielectric surfaces is a basic research topic in electromagnetics. It is the base of the well-known transition radiation (TR) [1,2] and diffraction radiation (DR) [3,4], which have broad application in present-day science and technology via providing powerful tools for producing electromagnetic emission [5,6] and for beam diagnostics [7,8]. Among these types of radiation, Smith-Purcell radiation (SPR) [9–11], which is a kind of coherent DR obtained using an electron beam to interact with a periodic surface, is especially noteworthy, since it affords a promising way of generating terahertz waves [12–15], which has diverse application prospects [16–18] and is difficult to realize by other means. However, in the conventional TR and SPR schemes, the efficiency of the beam-wave interaction is restricted essentially by the decay length of the induced field of the electron beam, which can be expressed as $\beta\gamma\lambda/4\pi$ [19], where λ is the wavelength of the radiation, and β and γ are the relativistic factors of the moving

electron. For TR, only a specified spot within the decay length around the interception point on the surface can emit radiation [20]. For SPR, only electrons with distances to the radiator surface that are less than the decay length can excite radiation [21,22]. In practice, an electron bunch with a relatively low energy (which is of most interest in the present paper thanks to its compactness and low cost) generally has a relatively large cross section due to the space-charge effect, so that a large portion of the electrons in the bunch are beyond the decay length and cannot efficiently interact with the radiator surface. In a word, either the radiator surface or the electron beam cannot be utilized sufficiently for generating electromagnetic radiation in the previous TR and SPR schemes.

To break through the restriction imposed by the decay length, here we propose to use a flat electron beam with a large cross section that is projected obliquely onto a metallic periodic surface, rather than passing over it in a parallel direction (see Fig. 1); by this means, all the electrons in the bunch can get close to and interact efficiently with the surface, and a large area of the surface of the structure can be excited by the electron beam to generate radiation, such that the overall efficiency is enhanced. In addition, in order to obtain coherent radiation from all of the functioning periodic surface, we use a one-dimensional metallic

*liuhao@nuaa.edu.cn

†liushg@sjtu.edu.cn

‡These authors contributed equally to this work.

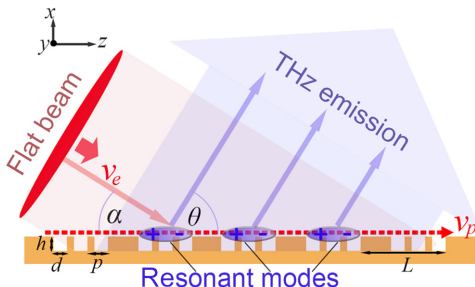


FIG. 1. Schematic diagram of radiation obtained using a metasurface to intercept an obliquely incident electron beam.

metasurface formed by an array of coupled grooves to replace an ordinary grating. As investigated in Ref. [23], a cluster of coupled grooves can form a set of Fabry-Perot (FP)-like resonating modes with a relatively high quality factor (compared with that of an uncoupled groove [24–26]), and an array of FP-like resonators can generate coherent DR with an enhanced intensity provided that the following constructive-interference condition is satisfied:

$$\omega \left(\frac{L}{v_p} - \frac{L \cos \theta}{c} \right) = \omega \left(\frac{L \cos \alpha}{v_e} - \frac{L \cos \theta}{c} \right) = 2n\pi, \quad (1)$$

where ω is the angular frequency, $v_p = v_e / \cos \alpha$ is the effective velocity of the electron beam along the surface [27], v_e is the electron velocity, α is the angle between the electron velocity and the grating, θ is the radiation direction, as shown in the figure, c is the speed of light in vacuum, and n is a positive integer indicating the coherence order. Equation (1) is a modified form of the well-known SPR relation, with the effective electron velocity v_p . We show that the radiation intensity obtained in the proposed scheme is remarkably higher than that for conventional SPR schemes, which use an electron beam to skim over a periodic surface in a direction parallel to the surface. Also, the intensity in this scheme is several orders of magnitude higher than that for conventional TR schemes and grating-based TR schemes, which use an electron beam to strike a planar surface and a periodic corrugated surface, respectively. Thus, it affords a promising option for the development of compact and high-power terahertz sources.

II. THEORY AND EXPERIMENT

Our investigation is based on a direct-current (dc) electron gun with a thermionic cathode, built by us at Shanghai Jiaotong University. A photograph and a sketch of the experimental setup are shown in Figs. 2(a) and 2(b), respectively. A dc electron beam is generated by the electron gun and is then focused in one of the transverse directions by using a set of coils. The operating voltage of the electron gun can be varied from 0 to 100 kV. After

being accelerated by the gun and being shaped by coils, the electron beam, with a flat cross section, is injected into a vacuum chamber, in which an adjustable platform carrying the designed radiating structures is located. The generated emission is output through a dielectric window in a direction perpendicular to the direction of motion of the beam, and is then detected by a Golay-cell detector. In other words, the direction of the detected radiation in the experiment is perpendicular to the electron velocity: $\alpha + \theta = 90^\circ$. According to Ref. [23], the radiation frequency of SPR from an array of FP-like resonators is determined by the FP-like mode excited in the coupled grooves, and the radiation direction is confined to specified directions determined by Eq. (1). Without loss of generality, three grooves are chosen in each cluster, and the structure parameters of the metasurface shown in Fig. 1 are set to $d = 0.09$ mm, $p = 0.13$ mm, $h = 0.12$ mm, and $L = 0.57$ mm. The calculated resonant frequency of the primary FP-like mode in the coupled grooves is about 0.44 THz, and the quality factor of the FP-like mode is about 70. In order to let the radiation direction defined by Eq. (1) be perpendicular to the direction of motion of the electrons, the operation voltage of the electron gun is chosen to be 32 kV, such that the beam velocity v_e is about $0.34c$.

In the experiment, the transverse size of the electron beam is measured by using a fluorescent screen, which is set on the adjustable platform, to intercept the electron beam at different longitudinal positions in the direction of motion of the beam. The measured beam sizes at several locations around the radiator are shown in Fig. 2(c). Here the operation voltage of the electron gun is 32 kV, and the dc beam current is about $0.1 \mu\text{A}$. We can see that an electron beam with a flat shape in its transverse section is realized. The width of the flat beam (the transverse beam size in the x' direction shown in the figure) is about 2 mm and is well within the range of a 20-mm length, within which the radiating components can be set for terahertz-wave generation. We perform theoretical analyses and experimental measurements based on this beam parameter, as presented in the following.

In principle, both SPR and TR can be generated by the proposed scheme, and the two should be considered separately. We first investigate them based on analytic derivations and numerical simulations. In the theoretical treatment of SPR, the mode-matching method is used [28]. Considering that the path of the electron beam is oblique, we first derive the incident fields of the electron beam in the beam-based coordinate system (x', y', z') and then transform them to the structure-based coordinate system (x, y, z). To obtain the total radiation excited by the flat electron beam, we first deal with the case of single-particle excitation and then perform an integration over a whole bunch [29,30] (the detailed derivations are given in the Appendix).

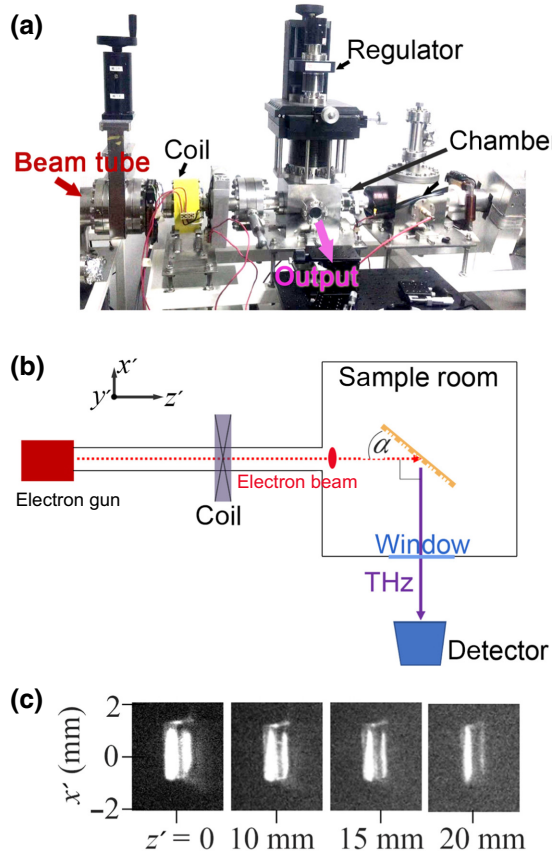


FIG. 2. (a) Photograph of the experimental setup. (b) Sketch of the experimental setup. (c) Bunch shape in the transverse direction measured at four positions along the direction of motion of the beam.

Simulations are performed by using a particle-in-cell code [31]. For the purposes of comparison, the following four cases are considered in the calculations and simulations: an inclined beam drives a metasurface (case I), a parallel beam drives a metasurface (case II), an inclined beam drives an ordinary grating with a large period L (case III), and an inclined beam drives an ordinary grating with a small period p (case IV). The calculated and simulated radiation spectra for the above four cases are presented in Figs. 3(a) and 3(b), respectively. Here the electron energy and the profile of the flat electron beam follow those in the experiment. The incidence angle α of the electron beam is 21° for the obliquely driven cases. In the analytic calculations, the metallic structure is treated as a perfect electric conductor, while in the simulations it is assumed to be a lossy metal with a conductivity of 1×10^7 S/m. As mentioned, both SPR and TR can be generated when an inclined electron beam is projected onto a metallic surface. However, both the calculated and the simulated results show that the intensity of the SPR is several orders of magnitude higher than that of the TR in our present model, which can be explained as follows. In order

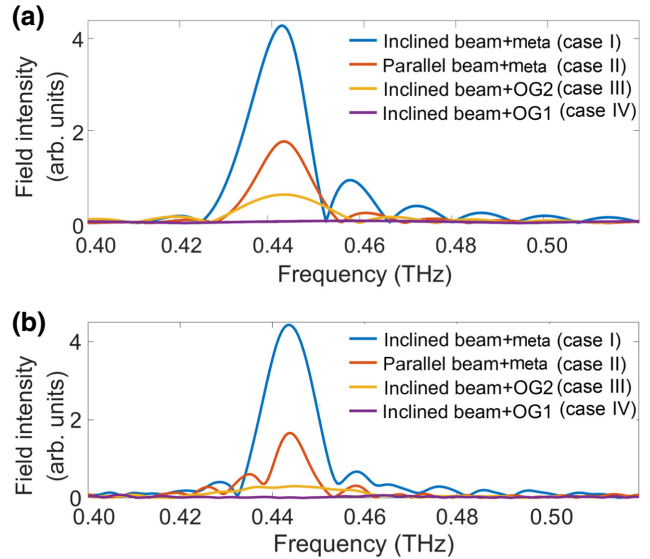


FIG. 3. (a) Calculated and (b) simulated radiation spectra for the four cases. Here, OG1 and OG2 denote ordinary gratings with periods of p and L , respectively.

to generate a high enough intensity of TR in the terahertz region, the electron energy generally needs to reach a level of several megaelectronvolts [6,30,32], orders of magnitude higher than that in our present experiment. In contrast, the electron energy required for generating SPR can be as low as several kiloelectronvolts [33]. Thus, SPR is the dominant emission in our present scheme. In the calculated results shown in Fig. 3(a), only SPR spectra are presented, while in the simulated results shown in Fig. 3(b), both SPR and TR are taken into consideration. We note that the simulated radiation spectra agree well with the theoretical ones. From both the calculated and the simulated results, we can see that the radiation from the metasurface reaches its highest peak at a frequency of 0.44 THz (see case I), coinciding with the oscillation frequency of the FP-like mode mentioned previously. The radiation intensity excited by the oblique beam is about 3 times higher than that excited by the parallel beam (see case II), indicating that the radiation power is about an order of magnitude higher. This can be explained by the fact that the decay length of a 32-keV electron beam is about 0.02 mm, much less than the bunch size, so that only a small portion of the parallel beam can interact efficiently with the metasurface [as illustrated in Fig. 4(b)], greatly reducing the overall radiation efficiency. From this figure, we can also see that the radiation intensities obtained from the ordinary gratings are remarkably lower than those obtained from the metasurfaces (see cases III and IV in the figure). In other words, the FP-like resonators in the metasurfaces play a vital role in generating enhanced radiation in the proposed scheme, as expected.

Figure 4 shows simulated field-contour maps (E_z component) at a frequency of 0.44 THz for the above four

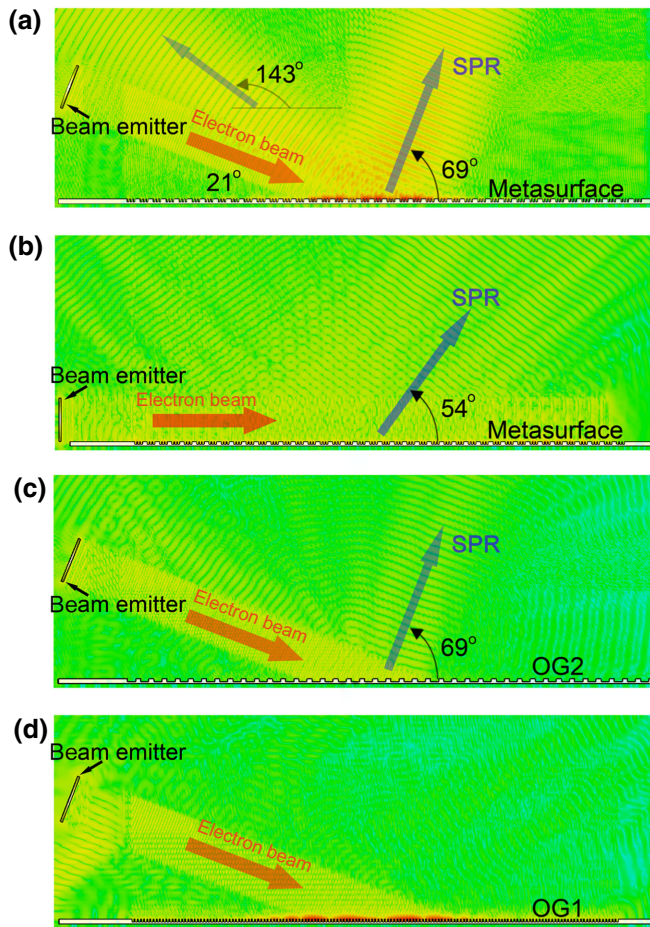


FIG. 4. Simulated contour maps of the E_z field for the four cases: (a) case I, (b) case II, (c) case III, and (d) case IV.

cases. From Fig. 4(a), we can see that in case I the radiation is mainly in the directions $\theta = 69^\circ$ and $\theta = 143^\circ$, which correspond to $n = 2$ and $n = 3$, respectively, in Eq. (1), for SPR. The intensity of the low-order radiation with $n = 2$ is much greater than that of the high-order radiation with $n = 3$ (here the coherence condition for the lowest order, with $n = 1$, is not satisfied), agreeing with the theoretical predictions. We note that the primary radiation direction ($\theta = 69^\circ$) is perpendicular to the beam velocity, namely, $\alpha + \theta = 90^\circ$, which is what we want in the experiment. Figure 1(b) shows that in case II, which uses a parallel beam to excite the metasurface, coherent SPR can also be generated, but the intensity is remarkably lower. Here the radiation direction changes to $\theta = 54^\circ$, because the effective velocity v_p of the inclined incident beam along the grating deviates from the actual beam velocity v_e , as indicated in Eq. (1). Figure 1(c) shows that in case III, which uses an inclined beam to drive an ordinary grating with a period of L , SPR can be generated, but the intensity is much lower than that obtained from the metasurface, while in case IV, with a period of p , SPR cannot be generated,

since the condition of Eq. (1) is not satisfied. Under this circumstance, TR is dominant, and the intensity is much weaker, as shown in Fig. 4(d).

In our experiment, we fabricate a metasurface and an ordinary rectangular grating with periods of p , as shown in Fig. 5(a). Here, the material of the metasurface and of the grating is chosen to be oxygen-free copper. Wire-electrode cutting techniques are used to fabricate the profiles of the structures. The structure parameters follow those used in the above calculations. We gradually change the angle α between the electron velocity and the metasurface from 0 to 60° ; the measured radiation intensity as a function of α is shown in Fig. 5(b), in which the theoretically calculated results are also presented for comparison. We note that the radiation intensity obtained from the metasurface reaches relative peak values at angles of $\alpha = 21^\circ$ and $\alpha = 47^\circ$, which correspond to the second ($n = 2$) and the third ($n = 3$) orders, respectively, of the coherent SPR at a frequency of 0.44 THz indicated in Eq. (1). In other words, coherent radiation from an array of FP-like modes with a resonant frequency around 0.44 THz is realized by use of the metasurface as predicted. The measured radiation intensity obtained from the metasurface is much higher than that from the ordinary grating, agreeing with the theoretical calculations. By using a standardized solid-state terahertz source to calibrate the Golay detector, the maximum measured radiation power from the metasurface is estimated to be about 10 nW.

Although this is higher than the measured power in other radiation schemes with a similar beam energy and current [34], this power level is not high enough for practical applications. The main determinant of the radiation power in practice is the beam current (or, more specifically, the functioning electron bunch charge). In the present experiment, the total bunch charge that simultaneously excites four periods of the metasurface (covered by the flat beam) is about 10^{-2} fC, which is not enough for generating high-power radiation. In practical implementations of the proposed scheme, the radiation power could be enhanced by increasing the functioning bunch charge, which could be done as follows. Firstly, a photocathode with a high emission current density could be used to replace the thermionic cathode used in the present experiment, as a result of which the present dc electron beam will be replaced by a short electron bunch with a high charge density. Secondly, a beam buncher could be used to longitudinally compress the electron bunch, realizing coherent radiation from the whole electron bunch with a high charge quantity. Figure 5(c) shows the calculated and simulated radiation power as the functioning bunch charge increases from 1 fC to 100 pC. We can see that the radiation power increases quadratically with the bunch charge, and the radiation power from the metasurface reaches hundreds of watts as the bunch charge reaches tens of picocoulombs, which can be readily obtained with

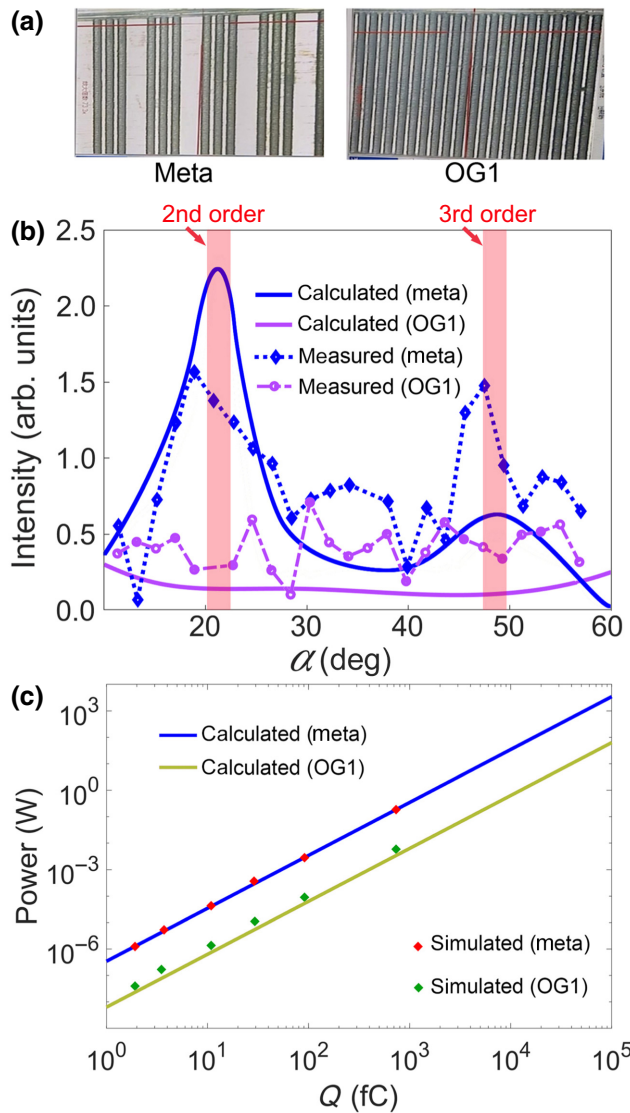


FIG. 5. (a) Enlarged images of the fabricated metasurface and grating. (b) Measured and calculated radiation intensity versus α . (c) Calculated and simulated radiation power versus functioning bunch charge. The calculated lines are quadratic curves.

available dc electron guns with photocathodes [35]. Hence, the proposed radiation scheme affords an effective option for developing compact and high-power terahertz sources.

III. CONCLUSION

In summary, we propose and investigate an enhanced coherent terahertz-wave generation scheme, which uses a metasurface formed by an array of Fabry-Perot-like resonant modes to obliquely intercept a low-energy flat electron beam with a large cross section. We demonstrate that the mechanism is a modified form of Smith-Purcell radiation rather than the expected transition radiation. The proposed scheme overcomes the restriction imposed by the

decay length and takes advantage of the Fabry-Perot-like resonators as well, greatly enhancing the radiation intensity. Hence, it provides an attractive option for developing compact and high-power terahertz sources.

ACKNOWLEDGMENTS

The authors gratefully acknowledge the support of the Natural Science Foundation of China under Grants No. U1632150, No. U1832185, No. 12075239, and No. 11675178.

APPENDIX: DERIVATION OF SMITH-PURCELL RADIATION AND TRANSITION RADIATION

In this appendix, we present derivations of the formulas for Smith-Purcell radiation and transition radiation from a metasurface formed by an array of groove clusters driven by an inclined incident flat electron beam.

We use the mode-matching method to deal with SPR, in which the space is divided into two regions according to the boundary conditions: region I (above the grooves) and region II (in the grooves). To obtain the diffraction radiation from a metasurface excited by a flat electron beam, we first deal with the case where a single particle excites a single cluster of grooves and then perform an integration over a whole electron bunch. Since the electron beam moves along an oblique line, we first derive the incident fields of the electron beam in the beam-based coordinate system (x', y', z') and then obtain the fields in the structure-based coordinate system (x, y, z) via coordinate transformation relations. In the (x', y', z') coordinate system, the incident fields of a uniformly moving particle consist of three components [28]: $E_{x'}^{\text{in}}$, $E_{z'}^{\text{in}}$, and H_y^{in} . The first two field components can be expressed in terms of $E_{z'}^{\text{in}}$, which satisfies the following nonhomogeneous wave equation in the (x', y', z') coordinate system [28,36]:

$$\frac{\partial^2 E_{z'}^{\text{in}}}{\partial x'^2} + \frac{\partial^2 E_{z'}^{\text{in}}}{\partial z'^2} - \frac{1}{c^2} \frac{\partial^2 E_{z'}^{\text{in}}}{\partial t^2} = \frac{1}{\epsilon_0} \frac{\partial \rho}{\partial z'} + \mu_0 \frac{\partial J_{z'}}{\partial t}. \quad (\text{A1})$$

Here ϵ_0 and μ_0 are the permittivity and permeability, respectively, of the vacuum, and ρ and J are the charge density and current density, respectively. For a particle with a quantity of charge q (per unit width in the y' direction) and with a velocity of v_e , we get [37]

$$\rho = q \delta(x' - x'_0) \delta(z' - v_e t) \quad (\text{A2})$$

and

$$J_{z'} = q v_{z'} \delta(x' - x'_0) \delta(z' - v_e t), \quad (\text{A3})$$

where δ is the Dirac delta function, and x'_0 denotes the transverse position of the particle in the x' direction. By

substituting Eqs. (A2) and (A3) into Eq. (A1) and applying the Fourier-transformation method, we can get the nonhomogeneous Helmholtz equation in the frequency domain,

$$\begin{aligned} \frac{\partial^2 E_{z'}^{\text{in}}(\omega)}{\partial x'^2} + \frac{\partial^2 E_{z'}^{\text{in}}(\omega)}{\partial z'^2} + k_0^2 E_{z'}^{\text{in}}(\omega) \\ = \frac{1}{\varepsilon_0} \frac{\partial \rho(\omega)}{\partial z'} - j\omega \mu_0 J_{z'}(\omega), \end{aligned} \quad (\text{A4})$$

where $k_0 = \omega/c$ and

$$\begin{aligned} \rho(\omega) &= \frac{1}{2\pi v} q\delta(x' - x'_0) e^{jk_{z0}z'}, \\ J_{z'}(\omega) &= \frac{1}{2\pi} q\delta(x' - x'_0) e^{jk_{z0}z'}, \end{aligned} \quad (\text{A5})$$

with $k_{z0} = \omega/v_e$. By solving Eq. (A4), we get

$$E_{z'}^{\text{in}}(\omega) = -\frac{jq\mu\omega}{4\pi\beta^2\gamma^2k_c} e^{-k_c|x'-x'_0|+jk_{z0}z'}, \quad (\text{A6})$$

where $k_c = \sqrt{k_{z0}^2 - k_0^2}$, and β and γ are the relativistic parameters of a moving particle. In the following, the parentheses in the expressions for the fields in the frequency domain are omitted for simplicity. Making use of Maxwell's equations, the other field components can be obtained:

$$H_y^{\text{in}} = \frac{q}{4\pi} \frac{x' - x'_0}{|x' - x'_0|} \exp(jk_{z0}z' - k_c|x' - x'_0|), \quad (\text{A7})$$

$$E_{x'}^{\text{in}} = \frac{q}{4\pi v\varepsilon_0} \frac{x' - x'_0}{|x' - x'_0|} \exp(jk_{z0}z' - k_c|x' - x'_0|). \quad (\text{A8})$$

Using the following coordinate transformation relations,

$$\begin{bmatrix} x' \\ y' \\ z' \end{bmatrix} = \begin{bmatrix} \cos\alpha & 0 & \sin\alpha \\ 0 & 1 & 0 \\ -\sin\alpha & 0 & \cos\alpha \end{bmatrix} \begin{bmatrix} x \\ y \\ z \end{bmatrix}, \quad (\text{A9})$$

and the following transformation relations for the electric field,

$$\begin{bmatrix} E_x \\ E_y \\ E_z \end{bmatrix} = \begin{bmatrix} \cos\alpha & 0 & -\sin\alpha \\ 0 & 1 & 0 \\ \sin\alpha & 0 & \cos\alpha \end{bmatrix} \begin{bmatrix} E_{x'} \\ E_{y'} \\ E_{z'} \end{bmatrix}, \quad (\text{A10})$$

we can then get the electromagnetic fields induced by an obliquely moving particle in the (x, y, z) coordinate

system:

$$E_z^{\text{in}}(x, z) = \frac{qR_0}{4\pi} \left[-\frac{j\omega\mu}{\beta^2\gamma^2k_c} \cos\alpha + \frac{1}{v\varepsilon} \frac{x \cos\alpha + z \sin\alpha}{|x \cos\alpha + z \sin\alpha|} \sin\alpha \right], \quad (\text{A11})$$

$$H_y^{\text{in}}(x, z) = \frac{qR_0}{4\pi} \frac{x \cos\alpha + z \sin\alpha}{|x \cos\alpha + z \sin\alpha|}, \quad (\text{A12})$$

where

$$R_0 = \exp[jk_{z0}(-x \sin\alpha + z \cos\alpha) - k_c|x \cos\alpha + z \sin\alpha|]. \quad (\text{A13})$$

The fields of the diffracted wave from a cluster of grooves in the (x, y, z) coordinate system can be written as follows:

$$\begin{aligned} E_z^{\text{I}} &= \int_{-\infty}^{+\infty} A(k_z^{\text{I}}) e^{jk_x^{\text{I}}x+jk_z^{\text{I}}z} dk_z^{\text{I}}, \\ E_x^{\text{I}} &= -\int_{-\infty}^{+\infty} \frac{k_z^{\text{I}}}{k_x^{\text{I}}} A(k_z^{\text{I}}) e^{jk_x^{\text{I}}x+jk_z^{\text{I}}z} dk_z^{\text{I}}, \\ H_y^{\text{I}} &= -\omega\varepsilon_0 \int_{-\infty}^{+\infty} \frac{1}{k_x^{\text{I}}} A(k_z^{\text{I}}) e^{jk_x^{\text{I}}x+jk_z^{\text{I}}z} dk_z^{\text{I}}, \end{aligned} \quad (\text{A14})$$

where $k_x^{\text{I}} = \sqrt{k_0^2 - k_z^{\text{I}}^2}$ and A is a coefficient to be determined from the boundary conditions.

In region II, the transmitted electromagnetic fields in the grooves can be expressed as [38,39]

$$\begin{aligned} E_z^{\text{II}} &= B_s \frac{\sin[k_0(x+h)]}{\sin(k_0h)}, \\ H_y^{\text{II}} &= j \sqrt{\frac{\varepsilon_0}{\mu}} B_s \frac{\cos[k_0(x+h)]}{\sin(k_0h)}, \end{aligned} \quad (\text{A15})$$

where B_s is a coefficient to be determined from the boundary conditions, and s indicates the number of groove in the cluster. At the apertures of the grooves ($x = 0$), the fields must satisfy the following boundary conditions [38,39]:

$$(E_z^{\text{in}} + E_z^{\text{I}})|_{x=0} = \begin{cases} E_z^{\text{II}}|_{x=0}, & z_s - d/2 \leq z \leq z_s + d/2, \\ 0, & \text{otherwise,} \end{cases} \quad (\text{A16})$$

$$\int_{z_s-d/2}^{z_s+d/2} H_y^{\text{I}} \Big|_{x=0} dz = \int_{z_s-d/2}^{z_s+d/2} H_y^{\text{II}} \Big|_{x=0} dz. \quad (\text{A17})$$

By substituting Eqs. (A11)–(A15) into Eqs. (A16) and (A17) and performing straightforward algebraic manipulations, we can obtain the coefficients A and B_s . The radiation

power (as a function of the radiation direction θ) from a cluster of grooves can then be obtained as

$$P_0 = \eta \left| \frac{\omega \varepsilon_0 d}{2\pi} \sin c \left(\frac{k_0 d \cos \theta}{2} \right) \sum_s B_s \exp(-jk_0 s p \cos \theta) \right|^2, \quad (\text{A18})$$

where d and p are the structural parameters shown in Fig. 1. Since the radiation power excited by a single particle changes with the transverse position (x'_0) of the particle, the radiation power excited by an electron bunch with a transverse charge distribution $f(x'_0)$ can be expressed as

$$P_b = \int_w P_0(x'_0) |f(x'_0)|^2 dx'_0, \quad (\text{A19})$$

where w denotes the size of the electron beam in the x' direction. In the calculations, we assume the electrons to be uniformly distributed in the x' direction.

Now we consider the radiation from a metasurface formed by an array of groove clusters. When the electron beam is obliquely intercepted by the metasurface, the width of the electron beam w decreases gradually. Based on this knowledge, the radiation power from an array of clusters can be obtained as

$$P_t = \sum_{m=1}^M P_{bm} |e^{jk_z w_m m L \cos \alpha - jk_0 m L \cos \theta}|^2, \quad (\text{A20})$$

where M denotes the total number of groove clusters that can be excited by the inclined electron beam, w_m indicates the width of the electron beam driving the m th groove cluster, and P_{bm} indicates the radiation power from the m th groove cluster, expressed by Eq. (A19) with w replaced by w_m .

To deal with TR, again we start from a single particle. According to analyses in the previous literature, the spectral-angular distribution of the backward TR intensity obtained from a planar metallic surface excited by a particle with a quantity of charge e can be expressed as [40]

$$\begin{aligned} \frac{d^2 W_0}{d\Omega d\omega} &= \frac{1}{c} \left(\frac{e \beta \sin \alpha}{\pi \cos \theta} \right)^2 \\ &\times \left[\frac{\cos^2 \theta + \beta |\cos \theta| \cos \alpha}{(1 + \beta |\cos \theta| \cos \alpha)^2 - (\beta \sin \theta \sin \alpha)^2} \right]^2. \end{aligned} \quad (\text{A21})$$

Here only the parallel polarization component is considered [30]. For a cluster of grooves, the spectral-angular

distribution reads

$$\frac{d^2 W_c}{d\Omega d\omega} = \frac{d^2 W_0}{d\Omega d\omega} \left| \sum_s \exp \left[js \omega p \left(\frac{\cos \alpha}{v} - \frac{\cos \theta}{c} \right) \right] \right|^2, \quad (\text{A22})$$

where s denotes the number of the groove in the cluster. Here the TR from the surfaces within the grooves is ignored. For an array of groove clusters, the radiation intensity can be expressed as a superposition of that from all the clusters:

$$\frac{d^2 W}{d\Omega d\omega} = \frac{d^2 W_c}{d\Omega d\omega} \left| \sum_{m=1}^M \exp \left[jm \omega L \left(\frac{\cos \alpha}{v} - \frac{\cos \theta}{c} \right) \right] \right|^2. \quad (\text{A23})$$

The total intensity of the TR excited by a single particle as a function of frequency can be obtained by integrating over all directions:

$$\frac{dW}{d\omega} = \int \frac{d^2 W}{d\Omega d\omega} d\Omega. \quad (\text{A24})$$

For an electron bunch with a specific charge distribution, the total intensity of the TR can be expressed as [41]

$$\frac{dW_t}{d\omega} = \frac{dW}{d\omega} N_e [1 + N_e f_b(\omega)]. \quad (\text{A25})$$

Here N_e is the total number of particles in the bunch, and $f_b(\omega)$ is the bunching factor determined by the charge distribution in the bunch.

-
- [1] U. Happek, A. J. Sievers, and E. B. Blum, Observation of Coherent Transition Radiation, *Phys. Rev. Lett.* **67**, 2962 (1991).
 - [2] Hung-chi Lihn, Pamela Kung, Chitrlada Settakorn, and Helmut Wiedemann, Observation of Stimulated Transition Radiation, *Phys. Rev. Lett.* **76**, 4263 (1996).
 - [3] A. P. Potylitsyn, M. I. Ryazanov, M. N. Strikhanov, and A. A. Tishchenko, *Diffraction Radiation from Relativistic Particles* (Springer-Velag, Berlin, 2009).
 - [4] T. Muto, S. Araki, R. Hamatsu, H. Hayano, T. Hirose, P. Karataev, G. Naumenko, A. Potylitsyn, and J. Urakawa, Observation of Incoherent Diffraction Radiation from a Single-Edge Target in the Visible-Light Region, *Phys. Rev. Lett.* **90**, 104801 (2003).
 - [5] P. Henri, O. Haeberle, P. Rullhusen, N. Maene, and W. Mondelaers, Grating transition radiation: A source of quasi-monochromatic radiation, *Phys. Rev. E* **60**, 6214 (1999).
 - [6] G. Naumenko, A. Aryshev, A. Potylitsyn, M. Shevelev, L. Sukhikh, N. Terunuma, and J. Urakawa, Monochromatic coherent grating transition radiation in sub-THz frequency range, *Nucl. Instrum. Methods B* **402**, 153 (2017).

- [7] M. Castellano, V. A. Verzilov, L. Catani, A. Cianchi, G. Orlandi, and M. Geitz, Measurements of coherent diffraction radiation and its application for bunch length diagnostics in particle accelerators, *Phys. Rev. E* **63**, 056501 (2001).
- [8] D. Mihalcea, C. L. Bohn, U. Happek, and P. Piot, Longitudinal electron bunch diagnostics using coherent transition radiation, *Phys. Rev. ST Accel. Beams* **9**, 092801 (2006).
- [9] S. J. Smith and E. M. Purcell, Visible light from localized surface charges moving across a grating, *Phys. Rev.* **92**, 1069 (1953).
- [10] J. Urata, M. Goldstein, M. F. Kimmitt, A. Naumov, C. Platt, and J. E. Walsh, Superradiant Smith-Purcell Emission, *Phys. Rev. Lett.* **80**, 516 (1998).
- [11] K. B. Oganesyan, Smith-Purcell radiation amplifier, *Laser Phys. Lett.* **12**, 116002 (2015).
- [12] W. Liu, L. Liang, Q. Jia, L. Wang, and Y. Lu, Multicolor Terahertz Frequency Mixer Using Multibunching of Free-Electron Beams, *Phys. Rev. Appl.* **10**, 034031 (2018).
- [13] J. Gardelle, P. Modin, H. P. Bluem, R. H. Jackson, J. D. Jarvis, A. M. M. Todd, J. T. Donohue, and " , A compact THz source: 100/200 GHz operation of a cylindrical Smith-Purcell free-electron laser, *IEEE Trans. THz Sci. Technol.* **6**, 1 (2016).
- [14] C. Prokop, P. Piot, M. C. Lin, and P. Stoltz, Numerical modeling of a table-top tunable Smith-Purcell terahertz free-electron laser operating in the super-radiant regime, *Appl. Phys. Lett.* **96**, 151502 (2010).
- [15] W. Liu and Z. Xu, Special Smith Purcell radiation from an open resonator array, *New J. Phys.* **16**, 073006 (2014).
- [16] M. Tonouchi, Cutting-edge terahertz technology, *Nat. Photonics* **1**, 97 (2007).
- [17] Lucy A. Downes, Andrew R. MacKellar, Daniel J. Whiting, Cyril Bourgenot, Charles S. Adams, and Kevin J. Weatherill, Full-Field Terahertz Imaging at Kilohertz Frame Rates Using Atomic Vapor, *Phys. Rev. X* **10**, 011027 (2020).
- [18] S. S. Dhillon, M. S. Vitiello, E. H. Linfeld, A. G. Davies, M. C. Hoffmann, J. Booske, C. Paoloni, M. Gensch, P. Weightman, G. P. Williams, *et al.*, The 2017 terahertz science and technology roadmap, *J. Phys. D: Appl. Phys.* **50**, 043001 (2017).
- [19] O. Haeberlé, P. Rullhusen, J. M. Salomé, and N. Maene, Calculations of Smith-Purcell radiation generated by electrons of 1–100 MeV, *Phys. Rev. E* **49**, 3440 (1994).
- [20] Y. Shibata, S. Hasebe, K. Ishi, T. Takahashi, T. Ohsaka, M. Ikezawa, T. Nakazato, M. Oyamada, S. Urasawa, T. Yamakawa, and Y. Kondo, Observation of coherent diffraction radiation from bunched electrons passing through a circular aperture in the millimeter- and submillimeter-wavelength regions, *Phys. Rev. E* **52**, 6787 (1995).
- [21] V. Kumar and K. J. Kim, Analysis of Smith-Purcell free-electron lasers, *Phys. Rev. E* **73**, 026501 (2006).
- [22] H. L. Andrews and C. A. Brau, Gain of a Smith-Purcell free-electron laser, *Phys. Rev. ST Accel. Beams* **7**, 070701 (2004).
- [23] W. Liu, Z. Yu, L. Sun, Y. Liu, Q. Jia, H. Xu, and B. Sun, Coherent terahertz emission from free-electron-driven Fabry-Pérot resonators with coupled grooves, *J. Phys. D: Appl. Phys.* **54**, 055104 (2021).
- [24] C. Fabry and A. Perot, Theorie et applications d'une nouvelle méthode de spectroscopie interréférentielle, *Ann. Chim. Phys.* **16**, 115 (1899).
- [25] W. Zhu, A. Agrawal, and A. Nahata, Planar plasmonic terahertz guided-wave devices, *Opt. Express* **16**, 6216 (2008).
- [26] L. Liang, W. Liu, Q. Jia, L. Wang, and Y. Lu, Multi-color and multidirectional-steerable Smith-Purcell radiation from 2D subwavelength hole arrays, *Appl. Phys. Lett.* **113**, 013501 (2018).
- [27] Y. Liu, W. Liu, L. Liang, Q. Jia, L. Wang, and Y. Lu, Threshold-less and focused Cherenkov radiations using sheet electron-beams to drive sub-wavelength hole arrays, *Opt. Express* **26**, 34994 (2018).
- [28] P. M. van den Berg, Smith-Purcell radiation from a line charge moving parallel to a reflection grating, *J. Opt. Soc. Am.* **63**, 689 (1973).
- [29] Y. Shibata, S. Hasebe, K. Ishi, S. Ono, M. Ikezawa, T. Nakazato, M. Oyamada, S. Urasawa, T. Takahashi, T. Matsuyama, and K. Kobayashi, Coherent Smith-Purcell radiation in the millimeter-wave region from a short-bunch beam of relativistic electrons, *Phys. Rev. E* **57**, 1061 (1998).
- [30] S. Pakluea, S. Rimjaem, J. Saisut, and C. Thongbai, Coherent THz transition radiation for polarization imaging experiments, *Nucl. Instrum. Methods Phys. Res. Sect. B* **464**, 28 (2020).
- [31] CST Corp., CST PS Tutorials, <http://www.cstchina.cn/>.
- [32] Y. Yu, K. Lai, J. Shao, J. Power, M. Conde, W. Liu, S. Doran, C. Jing, E. Wisniewski, and G. Shvets, Transition Radiation in Photonic Topological Crystals: Quasiresonant Excitation of Robust Edge States by a Moving Charge, *Phys. Rev. Lett.* **123**, 057402 (2019).
- [33] A. Massuda, C. Roques-Carmes, Y. Yang, S. E. Kooi, Y. Yang, C. Murdia, K. K. Berggren, I. Kaminer, and M. Soljacic, Smith-Purcell radiation from low-energy electrons, *ACS Photonics* **5**, 3513 (2018).
- [34] G. Adamo, K. F. MacDonald, N. I. Zheludev, Y. H. Fu, C. M. Wang, D. P. Tsai, and F. J. Garcia de Abajo, Light Well: A Tunable Free-Electron Light Source on a Chip, *Phys. Rev. Lett.* **103**, 113901 (2009).
- [35] B. M. Dunham and K. W. Smolenski, in *Proceedings of IEEE International Power Modulator and High Voltage Conference*, Atlanta GA, (2010), p. 98.
- [36] Jin Au Kong, *Electromagnetic Wave Theory* (EMW Publishing, Cambridge, Massachusetts, 2008).
- [37] D. Jackson, *Classical Electrodynamics* (Wiley, Hoboken, 1997).
- [38] Heinz Raether, *Surface Plasmons on Smooth and Rough Surfaces and on Gratings* (Springer-Velag, Berlin, 1988).
- [39] K. Zhang and D. Li, *Electromagnetic Theory in Microwave and Optoelectronics* (Springer-Velag, Berlin, 2008).
- [40] V. L. Ginzburg and V. N. Tsytovich, *Transition Radiation and Transition Scattering* (Hilger, Bristol, England, 1990).
- [41] Y. Shibata, K. Ishi, T. Takahashi, T. Kanai, F. Arai, S.-I. Kimura, T. Ohsaka, M. Ikezawa, Y. Kondo, R. Kato, S. Urasawa, T. Nakazato, S. Niwano, M. Yoshioka, and M. Oyamada, Coherent transition radiation in the far-infrared region, *Phys. Rev. E* **49**, 785 (1994).